European Congress on Computational Methods in Applied Sciences and Engineering
ECCOMAS 2004
P. Neittaanmäki, T. Rossi, S. Korotov, E. Oñate, J. Périaux, and D. Knörzer (eds.)
Jyväskylä, 24–28 July 2004

ACOUSTICS-CONVECTION UPSTREAM RESOLUTION ALGORITHMS FOR GAS DYNAMIC FLOWS

Joe Iannelli*

*City University
School of Engineering and Mathematical Sciences
Northampton Square
London EC1V 0HB, UK

Key words: CFD, Characteristics, Multi-dimensional Upwind, Implicit Formulation, Finite Elements, Shock-on-Shock Interaction

Abstract. *This paper details for the Euler and Navier-Stokes equations an intrinsically infinite-directional upstream formulation that rests on the mathematics and physics of multi-dimensional acoustics and convection. Based upon characteristic velocities, this formulation introduces the upstream bias directly at the differential equation level, before the spatial discretisation, within a characteristics-bias governing system. Through a decomposition of the Euler flux divergence into multi-dimensional acoustics and convection components, this characteristics-bias system induces consistent upstream bias along all directions of spatial wave propagation, with anisotropic variable-strength upstreaming that correlates with the spatial distribution of characteristic velocities. A conventional centered discretisation of this system on arbitrary grids directly yields an optimal discretely conservative and multi-dimensional upstream approximation for the Euler and Navier-Stokes equations. Even on relatively coarse grids, this method generates essentially non-oscillatory oblique- and interacting-shock solutions that preserve constant total enthalpy for adiabatic flows and mirror reference exact solutions.*

1 INTRODUCTION

This paper provides the first part of a two-part investigation into the development of continuum, i.e. non-discrete, multi-dimensional and infinite-directional characteristics-bias approximations of the Euler and Navier-Stokes equations. The second part [1], also presented at this conference, presents the spectral analysis of this formulation and applications to aerodynamic flows. This paper details the development of an acoustics-convection flux divergence decomposition and applications to the computational investigation of gas dynamic flows.

Multi-dimensional upwind Euler and Navier-Stokes solvers remain of considerable interest for computationally investigating realistic flows on arbitrary grids. Many finite element, difference and volume algorithms have progressed somewhat independently from the physics of acoustics and convection, the wave propagation mechanisms within gas dynamic flows. The dissipation mechanisms, or upwind schemes, within these algorithms have been developed at the discrete level, in connection with a specific grid or pattern of computational cells.

Several finite element solvers have either utilized modifications of the test space or introduced Taylor's series based dissipation terms to generate stable algorithms. The mathematical developments in these fundamental contributions have remained independent of characteristics theory. Upwind finite element methods for scalar equations have also been developed including the Streamline Upwind Petrov-Galerkin (SUPG) formulation, also known as the Streamline Diffusion (SD) method. Extensions to systems are recognized to remain heuristic, the induced upwinding is not necessarily in the streamline direction, and additional "shock capturing" terms are needed for computing essentially non-oscillatory shocked flows.

Intense research is also focused on multi-dimensional finite-volume upwind schemes that induce upwinding along a few significant directions. An early effort generated a grid-independent upwind scheme based on directional upwinding along possible shock wave directions. This approach later enjoyed addition of local Riemann solutions along several upwind directions including the flow velocity, speed gradient and pressure gradient directions. An alternative second order rotated upwind scheme used flux- difference splitting along two orthogonal directions determined on the basis of the pressure gradient. Other approaches involved approximate multi-dimensional Riemann solvers and local wave decompositions, with wave modelling. In these formulations, some wave directions and strengths are fixed a-priori to generate a viable CFD algorithm.

Difficulties remain in these methods both in assessing the magnitude of the induced multi-dimensional upwind diffusion and determining whether consistent upwinding exists not only over the selected directions, but along all flow-field wave- propagation directions. Additional data filtering or upwind-direction freezing may also be required for convergence and essential monotonicity. More fundamentally, current multi-dimensional upwind schemes are recognized to rest upon much less theoretical support than their

one-dimensional counterparts.

This two-part presentation expounds the multi-dimensional formulation of the acoustics-convection upstream resolution Euler solver detailed in [2]. Developed for the multi-dimensional Euler and Navier-Stokes equations with general equilibrium equations of state, this formulation develops the upstream-bias approximation directly at the differential equation level, before any discretisation. The formulation results in a "companion" characteristics-bias system that is associated with the governing equations and rests on a decomposition of the multi-dimensional Euler jacobian into acoustics and convection components. In particular, this analysis reveals that no single decomposition of the Euler flux components themselves can contain separate components that respectively correspond to the physics of multi-dimensional acoustics and convection.

This formulation induces the upstream bias along all flow-field directions of wave propagation and enjoys a consistent theoretical support that rests upon the mathematics and physics of multi-dimensional characteristic wave propagation. A traditional centered discretisation on arbitrary grids of the characteristics-bias system automatically and directly generates a consistent, discretely conservative and genuinely multi - dimensional upstream-bias approximation of the Euler and Navier-Stokes equations. The associated discrete multi - directional upstream-bias remains independent of the direction of the coordinate axes as well as orientation of each computational-cell side, which obviates the need for rotated stencils. This approximation requires data only from the computational cells shared by each grid node and also reduces to a consistent upstream approximation of the acoustics equations, for vanishing Mach number, which addresses the challenging problem of calculating low-Mach-number flows. Finite difference, volume, or element procedures can be used to discretise the characteristics-bias system. The algorithm in this paper has used a finite element discretisation.

The operation count for this algorithm is comparable to that of a simple flux vector splitting algorithm. The developments in this study have employed basic Lagrange four-noded cells. To determine the ultimate accuracy of bi-linear approximations of fluxes within four-noded cells, for a computationally efficient implementation, this study employs no MUSCL-type local extrapolation of dependent variables.

This paper is organized in 7 sections. After the introductory remarks in Section 1, Section 2 presents the reference multi-dimensional non-discrete upstream-bias formulation and Sections 3 delineates the Euler and Navier-Stokes equations. Section 4 details the development of the multi-dimensional acoustics-convection decomposition of the Euler flux divergence and Section 5 summarises the finite element discretisation of the characteristics-bias system. Section 6 discusses the numerical results, with concluding remarks presented in Section 7.

2 NON-DISCRETE UPSTREAM-BIAS APPROXIMATION

The non-discrete upstream-bias approximation is developed for the general non-linear parabolic system

$$\frac{\partial q}{\partial t} + \frac{\partial f_j(q)}{\partial x_j} - \frac{\partial f_j^\nu}{\partial x_j} = 0 \tag{1}$$

with implied summation on repeated subscript indices. This system reduces to a hyperbolic system when the term f_j^ν identically vanishes. For three-dimensional formulations, $1 \leq j \leq 3$, while the independent variable $(\boldsymbol{x}, t)$, $\boldsymbol{x} \equiv (x_1, x_2, x_3)$, in (1) varies in the domain $D \equiv \Omega \times [t_o, T]$, $[t_o, T] \in \mathcal{R}^+$, $\Omega \subset \mathcal{R}^n$, with $\mathcal{R}$ denoting the real-number field.

The non-discrete, i.e. continuum or before discretisation, upstream-bias approximation derives from a characteristics-bias integral statement associated with (1). The prototype integral statement is

$$\int_{\widehat{\Omega}} \widehat{w} \left(\frac{\partial q}{\partial t} + \frac{\partial f_j(q)}{\partial x_j} - \frac{\partial f_j^\nu}{\partial x_j} \right) d\Omega = 0 \tag{2}$$

which is equivalent to the governing system (1) for arbitrary smooth test functions $\widehat{w}$ with compact support in $\widehat{\Omega}$ and arbitrary subdomains $\widehat{\Omega} \subset \Omega$. The characteristics-bias integral is then defined as

$$\int_{\widehat{\Omega}} \widehat{w} \left(\frac{\partial q}{\partial t} + \frac{\partial f_j^C}{\partial x_j} - \frac{\partial f_j^\nu}{\partial x_j} \right) d\Omega = 0 \tag{3}$$

where f_j^C corresponds to a characteristics flux that automatically induces within (3) a multi-dimensional and infinite directional upstream-bias approximation for the hyperbolic flux divergence $\frac{\partial f_j}{\partial x_j}$. Most importantly, since the characteristics flux is developed independently and before any discretisation, a genuinely multi-dimensional upstream-bias approximation for the governing equations (1) on arbitrary grids directly results from a straightforward centered discretisation of the characteristics flux on the given grid.

To develop the flux f^C, consider first the flux jacobian decomposition (FJD) into L contributions

$$\frac{\partial f_j}{\partial q} = \sum_{\ell=1}^{L} \alpha_\ell \bar{A}_{\ell j} \quad \Rightarrow \quad \frac{\partial f_j}{\partial x_j} = \sum_{\ell=1}^{L} \alpha_\ell \bar{A}_{\ell j} \frac{\partial q}{\partial x_j} \tag{4}$$

where α_ℓ denotes a linear-combination function, possibly depending upon q, $\bar{A}_{\ell j}$ corresponds to a flux-jacobian matrix component such that the matrix $\bar{A}_{\ell j} n_j$ has uniform-sign eigenvalues within a conical region spanned by a unit vector $\boldsymbol{n}$, with components n_j, within the flow space.

An integral average of the Euler flux divergence $\frac{\partial f_j}{\partial x_j}$ as expressed through decomposition (4) becomes

$$\int_{\widehat{\Omega}} \widehat{w} \frac{\partial f_j}{\partial x_j} \, d\Omega = \int_{\widehat{\Omega}} \sum_{\ell=1}^{L} \widehat{w} \alpha_\ell \bar{A}_{\ell j} \frac{\partial q}{\partial x_j} \, d\Omega \tag{5}$$

The flux f_j^C is therefore defined by way of an upstream-bias integral average as

$$\int_{\widehat{\Omega}} \widehat{w} \frac{\partial f_j^C}{\partial x_j}\, d\Omega = \int_{\widehat{\Omega}} \sum_{\ell=1}^{L} (\widehat{w} + \bar{\psi}\delta_\ell \widehat{w})\, \alpha_\ell \bar{A}_{\ell j} \frac{\partial q}{\partial x_j}\, d\Omega \tag{6}$$

where the rhs integral provides an upstream bias for each matrix component within the FJD in (4).

The positive $\bar{\psi}$ in (6), $0 < \bar{\psi} < 1$, stands for an "upstream-bias" controller, which automatically adjusts the amount of induced upstream-bias diffusion, depending on local solution non-smoothness, [2]. The expression $\delta_\ell \widehat{w}$ denotes a directional variation of the test function $\widehat{w}$ along the axis of a conical region within the flow space. This variation induces the appropriate upstream-bias for the test function $\widehat{w}$ for each "ℓ" component within (6). Depending on the physical significance, magnitude and algebraic sign of the eigenvalues of $\bar{A}_{\ell j} n_j$, the variation $\delta_\ell \widehat{w}$ can vanish or become algebraically positive or negative, which corresponds to an upstream bias respectively in the negative or positive sense of the axis of each conical region.

Integration by parts of (6) and subsequent comparison with (5) generates the following expression for the divergence of the characteristics flux f_j^C

$$\frac{\partial f_j^C}{\partial x_j} = \frac{\partial f_j}{\partial x_j} - \frac{\partial}{\partial x_i}\left(\varepsilon \bar{\psi} \sum_{\ell=1}^{L} a_{i\ell} \alpha_\ell \bar{A}_{\ell j} \frac{\partial q}{\partial x_j} \right) \tag{7}$$

This expression exhibits an upstream-bias artificial diffusion, in the form of a second-order differential expression with associated upstream-bias matrix

$$\mathcal{A} \equiv n_i \left(\sum_{\ell=1}^{L} a_{i\ell} \alpha_\ell \bar{A}_{\ell j} \right) n_j \tag{8}$$

where n_i indicates the i^{th} direction cosine of a unit vector $\boldsymbol{n}$ along an arbitrary wave-propagation direction. For physical consistency of the upstream bias in (6), (7) and associated mathematical stability of the corresponding second-order differential expression, all the eigenvalues of this upstream-bias matrix must be positive at every flow-field point and for any wave-propagation direction $\boldsymbol{n}$. This requirement implies a consistent upstream bias along all directions radiating from any flow field point and thus becomes a fundamental upstream- bias stability condition.

3 EULER AND NAVIER STOKES EQUATIONS

With respect to an inertial Cartesian reference frame, the Navier-Stokes conservation law system is

$$\frac{\partial q}{\partial t} + \frac{\partial f_j(q)}{\partial x_j} - \frac{\partial f_j^\nu}{\partial x_j} = 0 \tag{9}$$

which consists of the continuity, linear-momentum and total-energy equations. In the absence of viscous stresses and heat conduction, the viscous-flow vector components f_j^ν vanishe and this system becomes the Euler system.

For 2-D flows, $1 \leq j \leq 2$ and the dependent-variable array $q = q(\boldsymbol{x}, t)$, and viscous and inviscid flux "vector" components f_j^ν, and $f_j = f_j(q)$ are then defined as

$$q \equiv \left\{ \begin{array}{c} \rho \\ m_1 \\ m_2 \\ E \end{array} \right\}, \quad f_1 \equiv \left\{ \begin{array}{c} m_1 \\ \frac{m_1}{\rho} m_1 + p \\ \frac{m_1}{\rho} m_2 \\ \frac{m_1}{\rho}(E+p) \end{array} \right\}, \quad f_2 \equiv \left\{ \begin{array}{c} m_2 \\ \frac{m_2}{\rho} m_1 \\ \frac{m_2}{\rho} m_2 + p \\ \frac{m_2}{\rho}(E+p) \end{array} \right\}, \quad f_j^\nu \equiv \left\{ \begin{array}{c} 0 \\ \tau_{1j} \\ \tau_{2j} \\ \frac{m_i}{\rho}\tau_{ij} - q_j^F \end{array} \right\} \tag{10}$$

In the array q, the variables ρ, m_1, m_2, and E, respectively denote static density and volume-specific linear momentum components and total energy. Concerning the viscous and inviscid fluxes, the variables τ_{ij}, q_j^F, and p respectively indicate the deviatoric stress-tensor components, the Fourier heat conduction flux component and static pressure. The Eulerian flow velocity $\boldsymbol{u}$, with cartesian components u_j, $1 \leq j \leq 2$, is then defined as $\boldsymbol{u} \equiv \boldsymbol{m}/\rho$.

The components τ_{ij} of the deviatoric stress tensor are expressed as

$$\tau_{ij} = \mu \left(\frac{\partial u_i}{\partial x_j} + \frac{\partial u_j}{\partial x_i} \right) + \lambda \frac{\partial u_\ell}{\partial x_\ell} \delta_i^j \quad , \quad \lambda = -\frac{2}{3}\mu + \eta_B \tag{11}$$

where δ_i^j indicates Kronecker's delta and μ and λ respectively denote the first and second coefficient of viscosity, and η_B indicates bulk viscosity. For monatomic gases η_B vanishes, while for other fluids, like air, Stokes' hypothesis $\lambda = -\frac{2}{3}\mu$ constitutes a reliable approximation.

The components q_j^F of the Fourier heat flux vector are expressed as

$$q_i = -k \frac{\partial T}{\partial x_i} \tag{12}$$

where T indicates static temperature and k denotes the coefficient of thermal conductivity.

The equations of state for p and T in terms of q are

$$p = (\gamma - 1) \left(E - \frac{1}{2\rho} \left(m_1^2 + m_2^2 \right) \right), \quad T = \frac{p}{\rho R} \tag{13}$$

with R denoting the gas constant. The square of the speed of sound c for general equations of state can be expressed as

$$c^2 \equiv \left. \frac{\partial p}{\partial \rho} \right|_S = p_\rho + p_E \left(\frac{E+p}{\rho} - \frac{1}{\rho^2} \left(m_1^2 + m_2^2 \right) \right) \tag{14}$$

in terms of the jacobian partial derivatives p_ρ and p_E of p. This result, in particular, allows expressing the mass-specific total enthalpy H as

$$H = \frac{E+p}{\rho} = \frac{c^2\left(1+p_E M^2\right) - p_\rho}{p_E} \tag{15}$$

where $M \equiv \|\boldsymbol{u}\|/c$ denotes the Mach number.

4 ACOUSTICS-CONVECTION CHARACTERISTICS EULER FLUX

The acoustics-convection flux jacobian decomposition consists of components that genuinely model the physics of multi-dimensional acoustics and convection. These components combine the computational simplicity of flux-vector splitting (FVS) with the accuracy and stability of flux-difference splitting (FDS) and also feature eigenvalues with uniform algebraic sign. This formulation eliminates the unstable linear-dependence problem in steady low-Mach-number flows and satisfies by design the upstream-bias stability condition. As the Mach number increases, the formulation smoothly approaches and then becomes an upstream-bias approximation of the entire flux divergence, along one single direction.

4.1 Convection and Pressure-Gradient Components

The flux divergence $\frac{\partial f_j}{\partial x_j}$ can be decomposed into convection and pressure-gradient components as

$$\frac{\partial f_j}{\partial x_j} = \frac{\partial f_j^q}{\partial x_j} + \frac{\partial f_j^p}{\partial x_j} \tag{16}$$

where f_j^q and f_j^p respectively denote the convection and pressure flux components, defined as

$$f_j^q(q) \equiv \begin{Bmatrix} m_j \\ \frac{m_j}{\rho} m_1 \\ \frac{m_j}{\rho} m_2 \\ \frac{m_j}{\rho}(E+p) \end{Bmatrix} = \frac{m_j}{\rho} \cdot \begin{Bmatrix} \rho \\ m_1 \\ m_2 \\ E+p \end{Bmatrix} \quad , \quad f_j^p(q) \equiv \begin{Bmatrix} 0 \\ p\delta_1^j \\ p\delta_2^j \\ 0 \end{Bmatrix} \tag{17}$$

For supersonic flows, the Euler eigenvalues associated with $\frac{\partial f_j}{\partial x_j}$ all have the same algebraic sign within a streamline wedge region and the entire flux divergence can be upstream approximated along the streamline principal direction, within this region. For subsonic flows these eigenvalues have mixed algebraic sign and an upstream approximation for the flux divergence along one single direction remains inconsistent with the two-way propagation of acoustic waves. Without the pressure gradient in the momentum equation, however, the corresponding flux-jacobian eigenvalues all have the same algebraic sign

within the streamline wedge region and the resulting convection flux divergence can then be upstream approximated along one single direction.

4.2 Acoustic Components

For arbitrary Mach numbers and corresponding dependent variables ρ, m_1, m_2 and E, the Euler flux Jacobians can be decomposed as

$$\frac{\partial f_j}{\partial q} = \frac{\partial f_j^q}{\partial q} + \frac{\partial f_j^p}{\partial q} = \frac{\partial f_j^q}{\partial q} + \bar{A}_j^a + \bar{A}_j^{nc} \tag{18}$$

where the matrices $\bar{A}_j^a$ and $\bar{A}_j^{nc}$ are defined as

$$\bar{A}_j^a \equiv \begin{pmatrix} 0 & , & \delta_1^j & , & \delta_2^j & , & 0 \\ p_\rho \delta_1^j & , & 0 & , & 0 & , & p_E \delta_1^j \\ p_\rho \delta_2^j & , & 0 & , & 0 & , & p_E \delta_2^j \\ 0 & , & \dfrac{c^2 - p_\rho}{p_E} \delta_1^j & , & \dfrac{c^2 - p_\rho}{p_E} \delta_2^j & , & 0 \end{pmatrix} \tag{19}$$

$$\bar{A}_j^{nc} \equiv \begin{pmatrix} 0 & , & -\delta_1^j & , & -\delta_2^j & , & 0 \\ 0 & , & p_{m_1} \delta_1^j & , & p_{m_2} \delta_1^j & , & 0 \\ 0 & , & p_{m_1} \delta_2^j & , & p_{m_2} \delta_2^j & , & 0 \\ 0 & , & -\dfrac{c^2 - p_\rho}{p_E} \delta_1^j & , & -\dfrac{c^2 - p_\rho}{p_E} \delta_1^j & , & 0 \end{pmatrix} \tag{20}$$

Heed, in particular that no flux component of $f_j(q)$ exists, of which the jacobian equals $\bar{A}_j^a$. For vanishing Mach numbers this matrix becomes the system matrix of the acoustics equations.

The eigenvalues of the matrix $\bar{A}_j^{nc} n_j$ have been determined in closed form as

$$\lambda_{1,3}^{nc} = 0 \quad , \quad \lambda_4^{nc} = -cMp_E v_j n_j \tag{21}$$

which become infinitesimal for vanishing M. The matrix $\bar{A}_j^{nc}$ can be termed a "non-linear coupling" matrix, for it completes the non-linear coupling between convection and acoustics within (18) so that the Euler eigenvalues can correspond to the sum of convection and acoustic speeds. Since the matrix $\bar{A}_j^a$ will be used in the upstream-bias formulation for small Mach numbers only and considering that the eigenvalues in (21) vanish for these Mach numbers and also for $\boldsymbol{n}$ pointing in the crossflow direction, for which $v_j n_j = 0$, no need exists to involve $\bar{A}_j^{nc}$ in the upstream-bias approximation of the flux jacobian.

The eigenvalues of $\bar{A}_j^a n_j$ have been exactly determined in closed form as

$$\lambda_{1,2}^a = 0 \quad , \quad \lambda_{3,4}^a = \pm\, c \tag{22}$$

and remain independent of the propagation vector $\boldsymbol{n}$, which signifies isotropic propagation. The matrix $\bar{A}_j^a$, therefore, can be termed the "acoustics" matrix, for its eigenvalues

approach the speed of sound c for decreasing Mach number. This matrix, therefore, can be used for an upstream-bias approximation of the Euler equations in the low Mach-number regime, within the streamline region, and for any Mach number, within the crossflow region.

For any two mutually perpendicular unit vectors $\boldsymbol{a} = (a_1, a_2)$ and $\boldsymbol{a}^N = (a_1^N, a_2^N)$ within a 2-D flow, along with implied summation on repeated indices, the acoustics component within the Euler flux divergence can be expressed as

$$\bar{A}_j^a \frac{\partial q}{\partial x_j} = \bar{A}_j^a a_j a_k \frac{\partial q}{\partial x_k} + \bar{A}_j^a a_j^N a_k^N \frac{\partial q}{\partial x_k} \tag{23}$$

For $\boldsymbol{a}$ parallel to $\boldsymbol{u}$, this expression corresponds to a decomposition of the Euler acoustics component into streamline and crossflow acoustics components. For wave-like solutions [1], two eigenvalues of each component vanish; the remaining eigenvalues of these separate components have been determined as

$$\lambda_{3,4}^s = \pm c a_j n_j \quad , \quad \lambda_{3,4}^N = \pm c a_j^N n_j \tag{24}$$

The two non-vanishing eigenvalues associated with the entire acoustics component at the lhs of (23), but as expressed as the rhs combination of streamline and crossflow components have then been determined as

$$\lambda_{3,4}^a = c \left(\left(a_j n_j \right)^2 + \left(a_j^N n_j \right)^2 \right)^{1/2} \quad , \quad \left(a_j n_j \right)^2 + \left(a_j^N n_j \right)^2 = 1 \tag{25}$$

which shows that the square of the acoustic eigenvalues (22) equals the sum of the square of the streamline and crossflow acoustic eigenvalues (24). For $\boldsymbol{a}$ and $\boldsymbol{a}^N$ respectively pointing in the streamline and crossflow directions, the Euler flux divergence can then be decomposed as

$$\frac{\partial f_j(q)}{\partial x_j} = \overline{\alpha} \bar{A}_j^a a_j a_k \frac{\partial q}{\partial x_k} + \bar{A}_j^a a_j^N a_k^N \frac{\partial q}{\partial x_k} + \frac{\partial f_j^q}{\partial x_j} + (1 - \overline{\alpha}) \bar{A}_j^a a_j a_k \frac{\partial q}{\partial x_k} + \bar{A}_j^{nc} \frac{\partial q}{\partial x_j} \tag{26}$$

The weights 1 and $\overline{\alpha}$, $1 \leq \overline{\alpha} \leq 0$, respectively for the crossflow and streamline components in this expression are different from each other because the streamline and crossflow characteristic velocity component remain different from each other, following the Euler eigenvalues, [1]. The magnitudes of needed acoustic upstream bias for (26) along these two directions, therefore, will have to differ from each other and this "differential" upstream bias can be easily instituted through the distinct weights $\overline{\alpha}$ and 1 on the streamline and crossflow components.

Despite its zero eigenvalues, $\bar{A}_j^a a_j$ features a complete set of eigenvectors X and thus possesses the similarity-transformation form

$$\bar{A}_j^a a_j = X \bar{\Lambda}^a X^{-1} = X \bar{\Lambda}^{a+} X^{-1} + X \bar{\Lambda}^{a-} X^{-1} \quad , \quad \bar{\Lambda}^a = \bar{\Lambda}^{a+} + \bar{\Lambda}^{a-} \tag{27}$$

The matrices $X\bar{\Lambda}^{a+}X^{-1}$ and $X\bar{\Lambda}^{a-}X^{-1}$ respectively correspond to the "forward" and "backward" acoustic-propagation matrix components of $\bar{A}^a_j a_j$. A bi-modal upstream-bias approximation of $\bar{A}^a_j a_j$, therefore, readily follows from instituting a forward and a backward upstream-bias approximation respectively for the forward- and backward-propagation matrices in (27). Results similar to (27) then readily follow by replacing $\boldsymbol{a}$ with $\boldsymbol{a}^N$. This bi-modal approximation directly yields both the non-negative-eigenvalue matrices

$$\left|\bar{A}^a_j a_j\right| \equiv X\left(\bar{\Lambda}^{a+} - \bar{\Lambda}^{a-}\right)X^{-1} = cI \quad , \quad \left|\bar{A}^a_j a^N_j\right| \equiv X_{_N}\left(\bar{\Lambda}^{a+} - \bar{\Lambda}^{a-}\right)X_{_N}^{-1} = cI \tag{28}$$

and the associated matrix product $\left|\bar{A}^a_j a_j\right| a_k \partial q/\partial x_k$, with I denoting the identity matrix. The matrices in (28) correspond to the streamline and crossflow absolute acoustics matrices.

4.3 Acoustics-Convection Flux Divergence Decomposition

The developments in the previous sections thus lead to the following acoustics-convection flux divergence decomposition

$$\begin{aligned}\frac{\partial f_j(q)}{\partial x_j} = \tilde{\alpha}\overline{\alpha}\left(X\bar{\Lambda}^{a+}X^{-1} + X\bar{\Lambda}^{a-}X^{-1}\right)a_k\frac{\partial q}{\partial x_k} + \tilde{\alpha}\left(X_{_N}\bar{\Lambda}^{a+}X_{_N}^{-1} + X_{_N}\bar{\Lambda}^{a-}X_{_N}^{-1}\right)a^N_k\frac{\partial q}{\partial x_k} + \\ + \left[\frac{\partial f^q_j}{\partial x_j} + (1-\tilde{\alpha}\overline{\alpha})\beta\frac{\partial f^p_j}{\partial x_j}\right] + (1-\tilde{\alpha}\overline{\alpha})(1-\beta)\frac{\partial f^p_j}{\partial x_j} + \\ + \tilde{\alpha}(\overline{\alpha}-1)\frac{\partial f^p_j}{\partial x_j} + \tilde{\alpha}\left(1-\overline{\alpha}\right)\bar{A}^a_j a_j a_k\frac{\partial q}{\partial x_k} + \tilde{\alpha}\bar{A}^{nc}_j\frac{\partial q}{\partial x_j}\end{aligned} \tag{29}$$

with $0 \leq \overline{\alpha}, \beta, \tilde{\alpha} \leq 1$.

4.4 Multi-dimensional Characteristics Euler Flux

With reference to (7), given the physical significance of the terms in decomposition (29) and algebraic signs of the corresponding eigenvalues, the associated principal direction unit vectors for these terms are

$$\boldsymbol{a}_1 = -\boldsymbol{a}_2 = \boldsymbol{a}_5 = -\boldsymbol{a}_6 = \boldsymbol{a} \quad , \quad \boldsymbol{a}_3 = -\boldsymbol{a}_4 = \boldsymbol{a}^N \quad , \quad \boldsymbol{a}_7 = \boldsymbol{a}_8 = \boldsymbol{a}_9 = \boldsymbol{0} \tag{30}$$

At each flow-field point, $\boldsymbol{a}$ and $\boldsymbol{a}^N$ remain respectively parallel and perpendicular to the local velocity, with $\boldsymbol{a}^N$ obtained by a 90^o-degree counterclockwise rotation of $\boldsymbol{a}$.

With (29), (30) along with the upstream-bias functions

$$\delta = (1-\tilde{\alpha}\overline{\alpha})(2\beta - 1) \quad , \quad \alpha = \tilde{\alpha}\overline{\alpha} \quad , \quad \alpha^N = \tilde{\alpha} \tag{31}$$

the general upstream-bias expression (7) directly yields the acoustics-convection characteristics flux divergence

$$\frac{\partial f_j^C}{\partial x_j} = \frac{\partial f_j}{\partial x_j} - \frac{\partial}{\partial x_i}\left[\varepsilon\bar{\psi}\left(c\left(\alpha a_i a_j + \alpha^N a_i^N a_j^N\right)\frac{\partial q}{\partial x_j} + a_i\frac{\partial f_j^q}{\partial x_j} + a_i\delta\frac{\partial f_j^p}{\partial x_j}\right)\right] \tag{32}$$

In this result, the expressions $\left(c\alpha a_i a_j\frac{\partial q}{\partial x_j} + a_i\frac{\partial f_j^q}{\partial x_j} + a_i\delta\frac{\partial f_j^p}{\partial x_j}\right)$ and $\left(c\alpha^N a_i^N a_j^N\frac{\partial q}{\partial x_j}\right)$ determine the upstream biases within respectively the streamline and crossflow wave propagation regions. These two expressions combined then induce a correct upwind bias along all wave propagation regions. In particular, the coupling of an upstream approximation for $(1-\alpha)\beta\frac{\partial f_j^p}{\partial x_j}$, via $\boldsymbol{a}_5$, with a downstream approximation for $(1-\alpha)(1-\beta)\frac{\partial f_j^p}{\partial x_j}$, via $\boldsymbol{a}_6$ results in an overall upstream approximation of the pressure gradient, but with variable weight δ. The operation count for expression (32) is then comparable to that of an FVS formulation. The terms in this expression, furthermore, directly correspond to the physics of acoustics and convection. Expression (32) determines f_i^C itself, up to an arbitrary divergence-free vector, as

$$f_i^C = f_i(q) - \varepsilon\bar{\psi}\left[c\left(\alpha a_i a_j + \alpha^N a_i^N a_j^N\right)\frac{\partial q}{\partial x_j} + a_i\frac{\partial f_j^q}{\partial x_j} + a_i\delta\frac{\partial f_j^p}{\partial x_j}\right] \tag{33}$$

According to this result, the intrinsic multi-dimensionality of each component f_i^C derives from its dependence upon the entire divergence of f_j^q and f_j^p.

For vanishing Mach numbers, α and α^N will approach 1 whereas δ will approach 0. Under these conditions, (32) reduces to

$$\frac{\partial f_j^C}{\partial x_j} = \frac{\partial f_j}{\partial x_j} - \frac{\partial}{\partial x_i}\left[\varepsilon\bar{\psi}\left(c\frac{\partial q}{\partial x_i} + a_i\frac{\partial f_j^q}{\partial x_j}\right)\right] \tag{34}$$

which essentially induces only an acoustics upstream bias. Heed that this bias becomes independent of specific propagation directions, for it no longer depends on $\left(\alpha a_i a_j + \alpha^N a_i^N a_j^N\right)$. This bias, therefore, becomes isotropic, in harmony with the isotropic propagation of acoustic waves. Observe, moreover, that the components within $\partial f_j^C/\partial x_j$ remain linearly independent of one another, which avoids the linear-dependence instability in the steady low-Mach-number Euler equations. For supersonic flows, $\alpha = 0$ and $\delta = 1$ and (32) thus becomes

$$\frac{\partial f_j^C}{\partial x_j} = \frac{\partial f_j}{\partial x_j} - \frac{\partial}{\partial x_i}\left[\varepsilon\bar{\psi}\left(c\alpha^N a_i^N a_j^N\frac{\partial q}{\partial x_j} + a_i\frac{\partial f_j}{\partial x_j}\right)\right] \tag{35}$$

which depends on the crossflow component of the absolute acoustics matrix and the entire divergence of the Euler inviscid flux vector.

5 FINITE ELEMENT WEAK STATEMENT

The divergence (32) of the characteristics flux f_j^C leads to the following characteristics-bias integral statement with implied summation on repeated subscript indices i, j

$$\int_\Omega w \left[\frac{\partial q}{\partial t} + \frac{\partial f_j}{\partial x_j} - \frac{\partial}{\partial x_i} \left(\varepsilon \bar{\psi} \left(c \left(\alpha a_i a_j + \alpha^N a_i^N a_j^N \right) \frac{\partial q}{\partial x_j} + a_i \frac{\partial f_j^q}{\partial x_j} + a_i \delta \frac{\partial f_j^p}{\partial x_j} \right) \right) \right] d\Omega = 0 \tag{36}$$

An integration by parts of the characteristics-bias expression then generates the weak statement

$$\int_\Omega \left[w \left(\frac{\partial q}{\partial t} + \frac{\partial f_j}{\partial x_j} \right) + \frac{\partial w}{\partial x_i} \varepsilon \bar{\psi} \left(c \left(\alpha a_i a_j + \alpha^N a_i^N a_j^N \right) \frac{\partial q}{\partial x_j} + a_i \frac{\partial f_j^q}{\partial x_j} + a_i \delta \frac{\partial f_j^p}{\partial x_j} \right) \right] d\Omega = 0 \tag{37}$$

where the surface integral on $\partial\Omega$ corresponding to the characteristics-bias expression vanishes because of the boundary condition $\bar{\psi}(\boldsymbol{x}_{\partial\Omega}) = 0$, imposed to eliminate unnecessary boundary upstream bias. The discrete equations then result from a finite element discretisation of this weak statement. An analogous statement applies to the Navier-Stokes equations.

The finite element weak statement associated with (37) is

$$\int_{\Omega^h} w^h \left(\frac{\partial q^h}{\partial t} + \frac{\partial f_j^h}{\partial x_j} \right) d\Omega +$$

$$+ \int_{\Omega^h} \frac{\partial w^h}{\partial x_i} \varepsilon^h \bar{\psi}^h \left(c^h \left(\alpha^h a_i^h a_j^h + \alpha^{N^h} a_i^{N^h} a_j^{N^h} \right) \frac{\partial q^h}{\partial x_j} + a_i^h \frac{\partial f_j^{q^h}}{\partial x_j} + a_i^h \delta^h \frac{\partial f_j^{p^h}}{\partial x_j} \right) d\Omega = 0 \tag{38}$$

where superscript "h" signifies spatial discrete approximation. The approximation q^h exists on a partition Ω^h, $\Omega^h \subseteq \Omega$, of Ω. This partition Ω^h has its boundary nodes on the boundary $\partial\Omega$ of Ω and results from the union of N_e non-overlapping elements Ω_e, $\Omega^h = \bigcup_{e=1}^{N_e} \Omega_e$. Within Ω^h, there exists a cluster of "master" elements Ω_k^M, each comprising only those adjacent elements that share a mesh node $\boldsymbol{x}_k$, with $1 \leq k \leq N$, where N denotes the total number of mesh nodes and hence master elements.

The discrete test function w^h within each master element Ω_k^M will coincide with the "pyramid" basis function $w_k = w_k(\boldsymbol{x})$, $1 \leq k \leq N$, with compact support on Ω_k^M. Such a function equals one at node $\boldsymbol{x}_k$, zero at all other mesh nodes and also identically vanishes both on the boundary segments of Ω_k^M not containing $\boldsymbol{x}_k$ and on the computational domain outside Ω_k^M.

In this study, each of the variables $\bar{\psi}^h$, α^h, c^h, $\boldsymbol{a}^h$, $\boldsymbol{a}^{N^h}$ and δ^h has been set equal to a piece wise constant for computational simplicity, one centroidal constant value per element. Likewise, ε^h is set equal to a reference length within each element, typically a measure of the element size. In this study, $\varepsilon^h = (\ell)_e/2$ within each element "e", where $(\ell)_e$ denotes the length of the streamline diameter of the generalized ellipse inscribed within

the element. The choice of a diameter in the streamline direction for $(\ell)_e$ rests on the recognition that the streamline is a characteristic principal direction, as discussed in [1].

Since the test and trial functions w_ℓ are prescribed functions of $\boldsymbol{x}$, the spatial integrations in (38) are directly carried out. For arbitrarily shaped elements, these integrations take place via the usual finite element local-coordinate transformation that for example maps a quadrilateral into a square. In this study, the resulting coordinate- transformation metrics within each element are set to constants equal to their respective centroidal values. This simplification allows the exact integration of the remaining integrals, which are then evaluated only once for each computation. Concerning the boundary variables, no extrapolation of variables is needed in this algorithm on a variable that is not constrained via a Dirichlet boundary condition. In this case, instead, the finite element algorithm (38) naturally generates for each unconstrained boundary variable a boundary-node ordinary differential equation.The complete integration with respect to $\boldsymbol{x}$ transforms (38) into a system of continuum-time ordinary differential equations (ODE) for determining at each time level t the unknown nodal values $q^h(\boldsymbol{x}_\ell, t)$, $1 \leq \ell \leq N$. This ODE system is numerically integrated in time via an implicit diagonal Runge-Kutta algorithm that remains absolutely stable for stiff non-linear dissipative systems, [2, 21]. The resulting linear algebra problems are solved via Gaussian elimination and GMRES.

6 Computational Results

The Acoustics-Convection Upstream Resolution Algorithm has generated essentially non-oscillatory results, as exemplified by solutions for a 2-D supersonic shock-on-shock interaction flow. The supersonic inlet corresponds to a free-stream Mach number $M_\infty = 2.40$, hence the inlet boundary conditions constrain density ρ, longitudinal and transversal linear momentum components m_1 and m_2 and total energy E. The outlet remains supersonic, hence no boundary conditions are enforced at this boundary. At the solid walls, the inviscid wall-tangency boundary condition is enforced. An initially uniform shockless flow is subject to deflections by an upper and a lower wall and the final steady state is computationally achieved by advancing the solution in time.

The finite element discretisation has employed Lagrange bilinear elements and the computational efficiency of the procedure has remained comparable to that of a conventional centered algorithm for the characteristics-bias system. As shown in Figure 1, the computational solution corresponds to a relatively coarse body -fitted grid of 40 bilinear elements in the transverse and longitudinal directions, for a total of 1600 elements, 1681 nodes and 6724 degrees of freedom. The upstream directions were continuously updated without any filtering or freezing, with high-rate convergence of the residual norm to 1×10^{-15}, hence machine zero, achieved in less than 60 time cycles at a constant maximum Courant number in excess of 100. The Mach-number flooded contours in the figure reveal the reflection of two interacting shocks. Figure 2 presents the Mach-number distribution. This distribution portrays a non-oscillatory solution with crisply captured shocks and plateaus. In particular, the reflected shocks are allowed to cross the boundary unperturbed, without

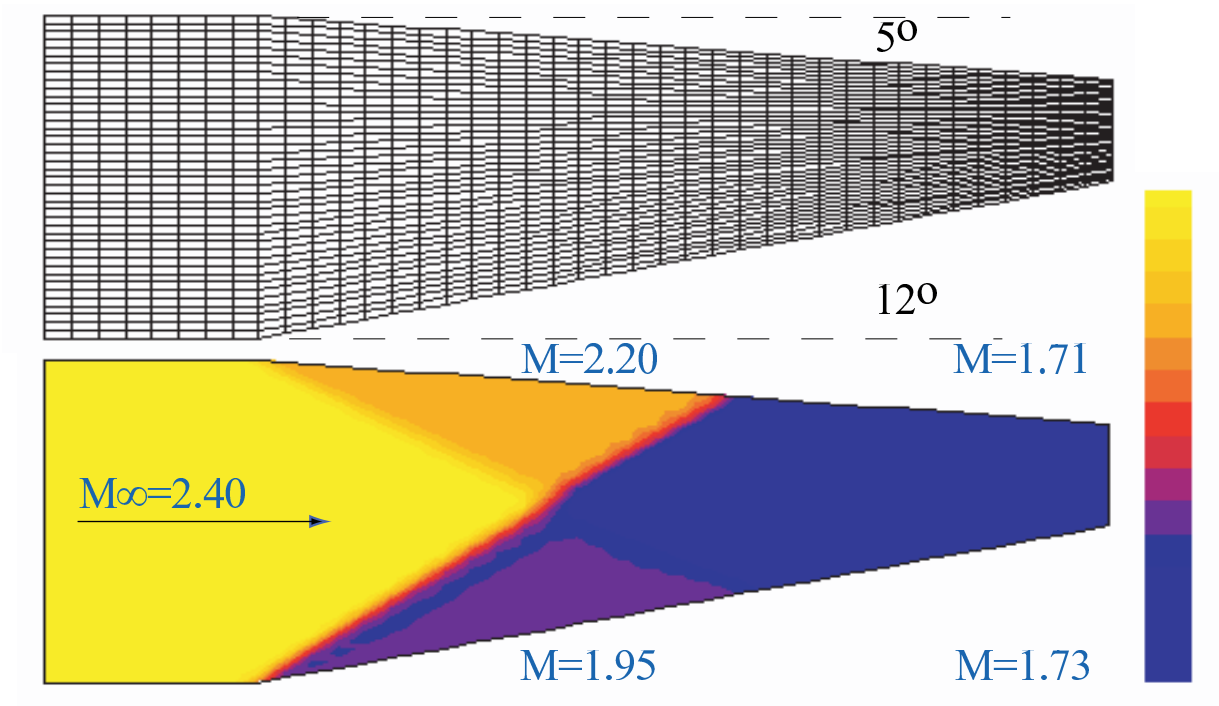

Figure 1: $M_\infty = 2.40$ Supersonic Shock-on-Shock Interaction, Computational Grid, Mach Number Field

any spurious distortion. Significantly, this computational solution essentially coincides with the available exact solution, with a calculated total enthalpy (15) that remains constant over the flow field, as is correct. Additional results are presented at the conference.

7 CONCLUDING REMARKS

The characteristics-bias upstream formulation rests upon the physics and mathematics of multi - dimensional characteristic acoustics and convection for general equations of state. It generates the upstream bias at the differential equation level, before any discrete approximation, by way of a characteristics-bias system and associated decomposition of the Euler flux divergence into convection and streamline and crossflow acoustic components.

A natural finite element discretisation of the characteristics-bias system directly provides a genuinely multi-dimensional upstream- bias approximation of the Euler equations. Along all the infinite directions of wave propagation, the formulation induces anisotropic and variable-strength consistent upwinding that correlates with the spatial distribution of characteristic velocities. The magnitude of the streamwise and crossflow upwind dissipations remain different from and independent of each other; the streamwise dissipation increases with the Mach number whereas the crossflow dissipation decreases with increas-

ing Mach number.

The developments in this investigation have implemented the algorithm using a linear approximation of fluxes within quadrilateral cells without any MUSCL-type local extrapolation of variables. This characteristics-bias algorithm admits a straightforward implicit implementation, features a computational simplicity that parallels a traditional centered discretisation, and rationally eliminates superfluous artificial diffusion. Even on relatively coarse grids, with continuously updated upstream directions and rapid convergence to steady state, this method generates essentially non-oscillatory oblique- and interacting-shock solutions that preserve constant total enthalpy for adiabatic flows and mirror reference exact solutions.

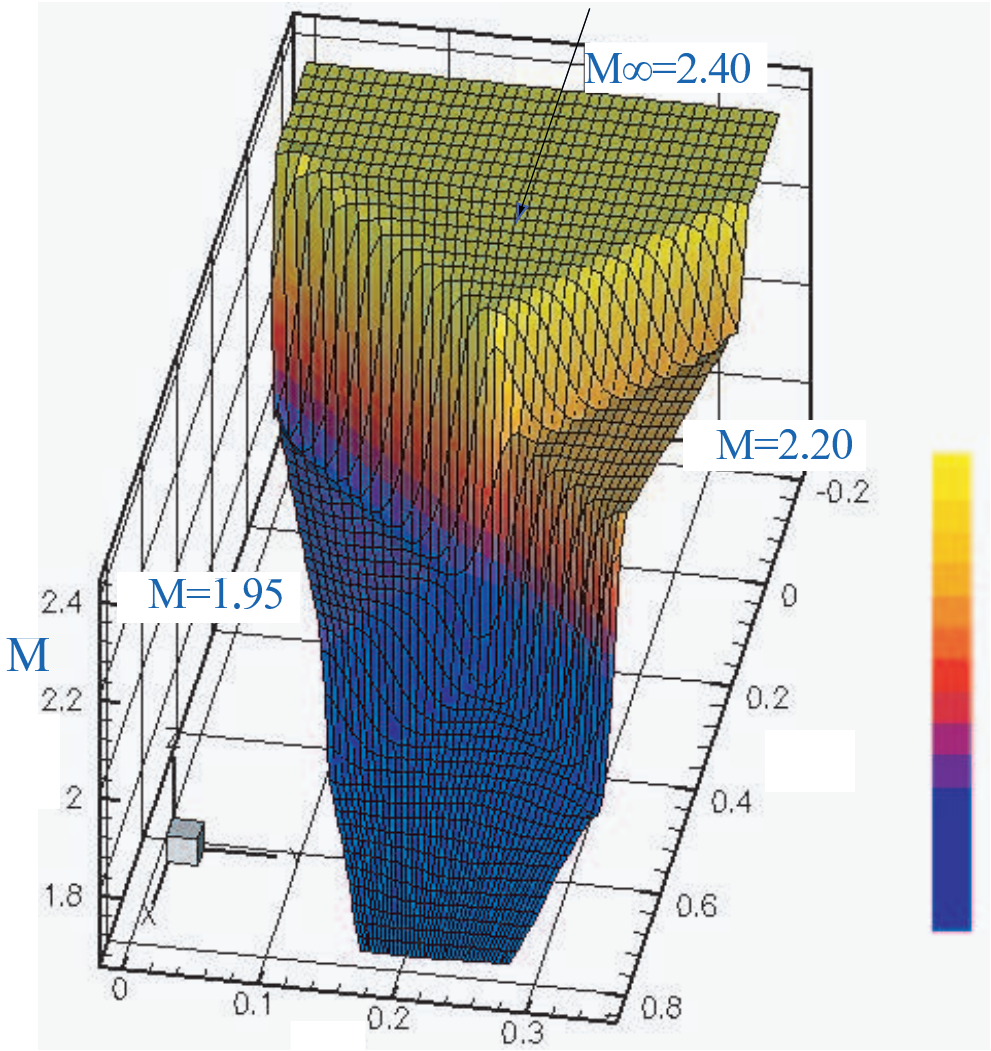

Figure 2: $M_\infty = 2.40$ Supersonic Shock-on-Shock Interaction, Mach Number Distribution

REFERENCES

[1] J. Iannelli "Spectral Analysis of an Acoustics-Convection Upstream Resolution Algorithm and Applications to Computational Aerodynamics", ECCOMAS 2004, (2004)

[2] J. Iannelli "A CFD Euler Solver from a Physical Acoustics-Convection Flux Jacobian Decomposition", Int. J. Numer. Meth. Fluids 31: 821-860 (1999)

[3] H. Luo, J. D. Baum, R. Löhner, J. Cabello, "Adaptive Edge-Based Finite Element Schemes for the Euler and Navier-Stokes Equations on Unstructured Grids", AIAA 93-0336 (1993).

[4] T. J. R. Hughes and A. Brooks, "A Theoretical Framework for Petrov-Galerkin Methods with Discontinuous Weighting Functions: Application to the Streamline-Upwind Procedure", Finite Elements in Fluids IV, 47-65, John Wiley, (1982).

[5] T. J. R. Hughes, "Recent Progress in the Development and Understanding of SUPG Methods with Special Reference to the Compressible Euler and Navier-Stokes Equations", International Journal for Numerical Methods in Fluids, 7, 11, (1987).

[6] C. Johnson, *Numerical Solution of Partial Differential Equations by the Finite Element Method*, Cambridge (1987).

[7] C. Johnson and Anders Szepessy, "On the Convergence of a Finite Element Method for a Nonlinear Hyperbolic Conservation Law", Mathematics of Computation, 49, 180, 427-444, (1987).

[8] C. Johnson, A. Szepessy, P. Hansbo, " On the Convergence of Shock-Capturing Streamline Diffusion Finite Element Methods for Hyperbolic Conservation Laws", Mathematics of Computation, 54, 189, 107-129, (1990).

[9] J.-C. Carette, H. Deconinck, H. Paillere, P. L. Roe, "Multidimensional Upwinding: Its Relation to Finite Elements", Inter. Journ. Numer. Meth. in Fluids, 20, 935-955, (1995).

[10] S.F. Davis, "A Rotationally-Biased Upwind Difference Scheme for the Euler Equations", Journal of Computational Physics 56, 65-92 (1984).

[11] D.W. Levy, K.G. Powell, and B. van Leer, "Use of a Rotated Riemann Solver for the Two-Dimensional Euler Equations", Journal of Computational Physics 106, 201-214 (1993).

[12] A. Dadone, and B. Grossman, "A Rotated Upwind Scheme for the Euler Equations", AIAA 91-0635 (1991).

[13] W. Coirier and B. van Leer, "Numerical Flux Formulas for the Euler and Navier-Stokes Equations: II. Progress in Flux-Vector Splitting", AIAA-91-1566, (1991).

[14] C. L. Rumsey, B. van Leer, P. L. Roe, " A Multidimensional Flux Function with Applications to the Euler and Navier-Stokes Equations" Journal of Computational Physics 105, 306-323 (1993).

[15] I. H. Parpia, "A Planar Oblique Wave Model for the Euler Equations" AIAA-91-1545-CP, (1991).

[16] H. Paillere, H. Deconinck, R. Struijs, P. L. Roe, L.M. Mesaros, J.D. Muller, "Computations of Inviscid Compressible Flows Using Fluctuation-Splitting on Triangular Meshes", AIAA 93-3301, (1993).

[17] P. L. Roe, "Beyond the Riemann Problem: Part I", in *Algorithmic Trends in CFD*, Springer Verlag (1993).

[18] C. Hirsch, *Numerical Computation of Internal and External Flows*, Vol. 1, 2 John Wiley & Sons, New York, NY, (1991).

[19] P. R. Garabedian, *Partial Differential Equations*, Chelsea Publishing Company, New York, N. Y., (1986).

[20] E. Zauderer, *Partial Differential Equations of Applied Mathematics*, John Wiley, New York, N. Y., (1989).

[21] K. Dekker and J.G. Verwer, *Stability of Runge-Kutta Methods for Stiff Non-Linear Differential Equations*, Elsevier Publishers, Amsterdam, (1984).